

Archival Report

Somatosensory-Motor Dysconnectivity Spans Multiple Transdiagnostic Dimensions of Psychopathology

Valeria Kebets, Avram J. Holmes, Csaba Orban, Siyi Tang, Jingwei Li, Nanbo Sun, Ru Kong, Russell A. Poldrack, and B.T. Thomas Yeo

ABSTRACT

BACKGROUND: There is considerable interest in a dimensional transdiagnostic approach to psychiatry. Most transdiagnostic studies have derived factors based only on clinical symptoms, which might miss possible links between psychopathology, cognitive processes, and personality traits. Furthermore, many psychiatric studies focus on higher-order association brain networks, thereby neglecting the potential influence of huge swaths of the brain.

METHODS: A multivariate data-driven approach (partial least squares) was used to identify latent components linking a large set of clinical, cognitive, and personality measures to whole-brain resting-state functional connectivity patterns across 224 participants. The participants were either healthy ($n = 110$) or diagnosed with bipolar disorder ($n = 40$), attention-deficit/hyperactivity disorder ($n = 37$), schizophrenia ($n = 29$), or schizoaffective disorder ($n = 8$). In contrast to traditional case-control analyses, the diagnostic categories were not used in the partial least squares analysis but were helpful for interpreting the components.

RESULTS: Our analyses revealed three latent components corresponding to general psychopathology, cognitive dysfunction, and impulsivity. Each component was associated with a unique whole-brain resting-state functional connectivity signature and was shared across all participants. The components were robust across multiple control analyses and replicated using independent task functional magnetic resonance imaging data from the same participants. Strikingly, all three components featured connectivity alterations within the somatosensory-motor network and its connectivity with subcortical structures and cortical executive networks.

CONCLUSIONS: We identified three distinct dimensions with dissociable (but overlapping) whole-brain resting-state functional connectivity signatures across healthy individuals and individuals with psychiatric illness, providing potential intermediate phenotypes that span across diagnostic categories. Our results suggest expanding the focus of psychiatric neuroscience beyond higher-order brain networks.

Keywords: Cognitive dysfunction, Impulsivity, Phenotypes, Psychopathology, Resting-state functional connectivity, Somatosensory-motor

<https://doi.org/10.1016/j.biopsych.2019.06.013>

Substantial overlap in clinical symptoms (1,2), cognitive deficits (3), genetic risk factors (4) across psychiatric disorders, and high comorbidity rates (5) suggest that current categorical classifications might not be carving nature by its joints. In response, transdiagnostic initiatives, such as the Research Domain Criteria (6,7) and the Hierarchical Taxonomy of Psychopathology (8,9), have worked toward new dimensionally oriented approaches by integrating findings from genetics, neuroimaging, and cognitive science.

Many recent transdiagnostic studies have derived latent dimensional factors that best explain the structure of psychopathology along with associated neural correlates. One example is the general psychopathology (or p) factor (10–15), which is thought to reflect individuals' susceptibility to develop "any and all forms of common psychopathologies" (16). The

p factor has been extended to other clinical dimensions, such as internalizing and externalizing symptoms (10,11,17,18). Importantly, these factors were extracted from the general population, supporting the idea that psychopathology lies on a spectrum spanning healthy and disease states. However, most studies have focused on deriving factors based only on clinical symptoms, which might be insensitive to intricate links between psychopathology, cognitive processes, and personality traits. Therefore, considering a broader set of behavioral measures might provide a more comprehensive characterization of individuals' phenotypic variability across mental health and disease.

Resting-state functional magnetic resonance imaging (rs-fMRI) is widely used to measure intrinsically organized patterns of spontaneous signal fluctuations (19), commonly referred to

as resting-state functional connectivity (RSFC). Because many psychiatric disorders are characterized by disturbances of large-scale brain network organization (20), RSFC might be a powerful tool for understanding transdiagnostic dimensions. Indeed, studies have found significant overlap in neural circuits altered in different disorders, suggesting common neurobiological mechanisms (21–25). RSFC alterations in higher-order (e.g., default mode, executive) networks are also associated with the *p* factor (14) or clinical symptoms (17,26). However, many psychiatric imaging studies have focused on higher-order association networks (20,27), neglecting the potential influence of huge swaths of cortex. Indeed, complex clinical and behavioral phenotypes arise from coordinated interactions throughout the entire connectome (28–30), suggesting the importance of examining whole-brain connectivity without prior assumptions.

Here, we used data from the University of California, Los Angeles (UCLA) Consortium for Neuropsychiatric Phenomics (CNP) (31), a unique dataset in which the imaging and behavioral assessment were focused on working memory and inhibitory control, two domains that are exceedingly relevant in multiple psychiatric disorders. This allowed us to consider behavioral phenotypes beyond the clinical symptoms typically examined in many transdiagnostic studies (10,11,14,15,17). Using a multivariate data-driven approach, we extracted latent components (LCs) that simultaneously link a large set of behavioral measures spanning clinical, cognitive, and personality domains with whole-brain RSFC patterns across healthy control individuals (HCs) and individuals with schizophrenia (SZ), schizoaffective disorder (SZAD), bipolar I disorder (BD), or attention-deficit/hyperactivity disorder (ADHD). This approach yielded dimensional components present in varying degrees among individuals as opposed to assigning each individual to a single categorical biotype (12,32). Furthermore, in contrast to traditional case-control analyses, the diagnostic labels were not utilized in the analysis but were used to interpret the behavioral-RSFC dimensions post hoc.

Our analyses revealed three transdiagnostic components corresponding to general psychopathology, cognitive dysfunction, and impulsivity. Each component was associated with a unique whole-brain RSFC pattern, such that interindividual variation in the expression of the three RSFC configurations captured individuals' variability along these behavioral dimensions. Strikingly, the three components all featured altered connectivity within the somatosensory-motor (somatomotor) system and in its connections to subcortical and cortical executive networks. Overall, this study identified three LCs as likely transdiagnostic phenotypes, thereby offering a putative model for explaining comorbidity across disorders. Our results add further evidence to the importance of considering a broad range of behavioral measures and expanding the focus of psychiatric neuroscience beyond higher-order association networks.

METHODS AND MATERIALS

Participants

We downloaded the UCLA CNP dataset from the public database OpenfMRI (33). The CNP dataset (31) comprised multimodal imaging and behavioral data from 272 participants,

including 130 HCs, 49 patients with BD, 43 patients with ADHD, 39 patients with SZ, and 11 patients with SZAD. These four disorders were selected by the CNP because they all were thought to involve some degree of impairment in response inhibition and memory mechanisms (34). See *Supplemental Methods* for details about participant recruitment.

After receiving a verbal explanation of the study, participants gave written informed consent following procedures approved by the Institutional Review Boards at UCLA and the Los Angeles County Department of Mental Health.

Clinical and Behavioral Assessment

All participants underwent a semistructured assessment with the Structured Clinical Interview for the DSM-IV-Text Revision (35). Demographic and clinical data for each group are summarized in *Table 1*.

The CNP behavioral assessment included an extensive set of clinical, cognitive, and personality scores (listed in *Supplemental Table S1*). We excluded behavioral measures from the partial least squares (PLS) analysis when scores were missing for at least 1 participant among the 224 participants who survived MRI preprocessing quality controls (see below).

A final set of 54 behavioral and self-report measures from 19 clinical, cognitive, and psychological tests were included in the PLS analysis. Behavioral measures for each group are shown in *Supplemental Table S2*. Notably, most clinical measures were excluded from the PLS analysis because they had not been administered to healthy individuals. However, excluded behavioral measures were considered in post hoc analyses (*Supplemental Table S3*).

MRI Acquisition and Processing

Structural and functional MRI data were acquired on two 3T Siemens Trio scanners (Siemens, Erlangen, Germany) at UCLA. fMRI acquisition comprised an rs-fMRI scan and seven fMRI tasks. See *Supplemental Methods* for details.

Of the 272 participants, 7 participants did not have an anatomical scan, 4 participants did not have an rs-fMRI scan, and 1 participant had signal dropout in the cerebellum (36), resulting in 260 participants undergoing preprocessing. The neuroimaging data were processed using a previously published pipeline (37,38). The pipeline code is available at https://github.com/ThomasYeoLab/CBIG/tree/master/stable_projects/preprocessing/CBIG_fMRI_Prepoc2016.

Structural MRI data were processed using FreeSurfer 5.3.0, a suite of automated algorithms for reconstructing accurate surface mesh representations of the cortex from individual participants' T1 images (39–42). The cortical surface meshes were then registered to a common spherical coordinate system (43,44).

rs-fMRI data were preprocessed with the following steps: 1) removal of the first four frames, 2) slice time correction with FSL (45,46), and 3) motion correction using rigid body translation and rotation with FSL. The structural and functional images were aligned using FsFast boundary-based registration (47). Framewise displacement (48) and root mean square of voxelwise differentiated signal (DVARS) (49) were computed using *fsl_motion_outliers*. Volumes with framewise displacement > 0.2 mm or DVARS > 50 were marked as outliers

Table 1. Demographic and Clinical Data for Each Diagnostic Group

| | HC (n = 110) | ADHD (n = 37) | BD (n = 40) | SZ (n = 29) | SZAD (n = 8) | F or χ^2 | p Value |
|---|--------------|---------------|--------------|--------------|--------------|---------------|------------------------|
| Demographics | | | | | | | |
| Age, years, mean (SD) | 31.26 (8.66) | 31.22 (10.11) | 34.78 (9.24) | 35.59 (9.27) | 35.38 (8.94) | 2.34 | 5.6×10^{-2} |
| Female sex, n (%) | 53 (48) | 17 (46) | 17 (43) | 4 (14) | 4 (50) | 11.60 | 2.1×10^{-2} |
| Education, years, mean (SD) | 15.19 (1.59) | 14.57 (1.85) | 14.43 (1.91) | 12.62 (1.47) | 13.38 (1.77) | 14.49 | 1.6×10^{-10a} |
| Site 1, n (%) | 89 (81) | 19 (51) | 18 (45) | 13 (45) | 4 (50) | 27.74 | 1.4×10^{-5a} |
| Head Motion | | | | | | | |
| FD, mean (SD) ^b | 0.06 (0.03) | 0.06 (0.03) | 0.07 (0.03) | 0.08 (0.03) | 0.09 (0.05) | 3.50 | 8.5×10^{-3a} |
| Lifetime Substance Use ^c | | | | | | | |
| 0 substance, n (%) | 69 (63) | 15 (41) | 6 (15) | 9 (31) | 2 (25) | 32.38 | 1.6×10^{-6a} |
| 1 substance, n (%) | 24 (22) | 11 (30) | 8 (20) | 5 (17) | 0 (0) | 4.06 | 4.0×10^{-1} |
| 2+ substances, n (%) | 17 (15) | 11 (30) | 26 (65) | 15 (52) | 6 (75) | 44.65 | 4.7×10^{-9a} |
| No. substances, mean (SD) | 0.62 (1.04) | 1.32 (1.63) | 2.73 (2.11) | 2.07 (2.15) | 3.00 (2.51) | 16.67 | 6.1×10^{-12a} |
| Current Medication (by Target) ^d | | | | | | | |
| Dopaminergic, n (%) | 0 (0) | 10 (27) | 17 (42) | 19 (66) | 6 (75) | 44.80 | 1.9×10^{-27a} |
| Serotonergic, n (%) | 0 (0) | 2 (5) | 14 (35) | 17 (59) | 2 (25) | 71.14 | 1.6×10^{-38a} |
| GABAergic, n (%) | 0 (0) | 2 (5) | 13 (32) | 5 (17) | 0 (0) | 13.50 | 7.4×10^{-10a} |
| Glutamatergic, n (%) | 0 (0) | 1 (3) | 13 (32) | 3 (10) | 2 (25) | 25.11 | 3.9×10^{-17a} |
| Norepinephreric, n (%) | 0 (0) | 10 (27) | 14 (35) | 9 (31) | 4 (50) | 16.64 | 6.4×10^{-12a} |
| Others, n (%) | 0 (0) | 1 (3) | 5 (12) | 5 (17) | 1 (12) | 4.87 | 8.8×10^{-4a} |
| No. medications, mean (SD) | 0 (0) | 0.59 (1.14) | 2.33 (1.85) | 2.00 (1.51) | 2.50 (1.77) | 47.19 | 1.4×10^{-28a} |

Groups were compared with either analyses of variance (for continuous measures) or chi-square tests (for categorical measures).

ADHD, attention-deficit/hyperactivity disorder; BD, bipolar disorder; FD, framewise displacement; GABA, gamma-aminobutyric acid; HC, healthy control; SZ, schizophrenia; SZAD, schizoaffective disorder.

^ap Value that survived false discovery rate correction ($q < .05$).

^bFramewise displacement was computed as per Kong et al. (37).

^cLifetime substance use included substance abuse and/or dependence for nicotine, alcohol, cannabis, cocaine, amphetamine, sedatives/hypnotics/anxiolytics, inhalants, opioids and hallucinogens.

^dMedication was sorted by the neurotransmitter system(s) targeted by the medication currently used by participants, based on the Neuroscience-based Nomenclature [NbN-2 (86,87)] (<http://nbn2r.com/>). The full list of medications and their categorization can be found in Supplemental Table S4. Note that percentages do not add up to 100% because individuals often take more than one medication.

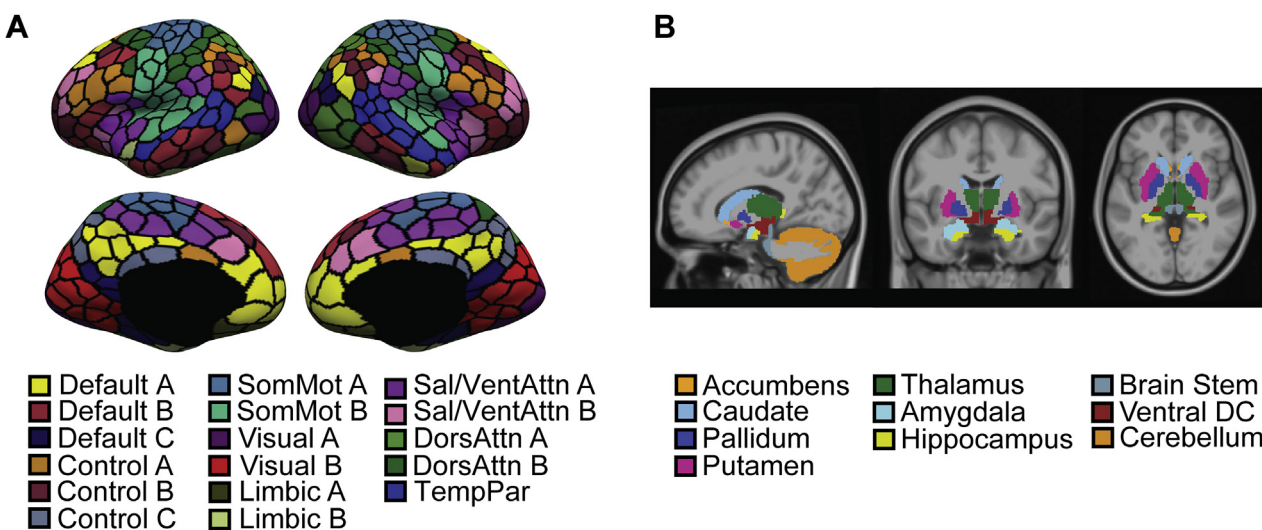
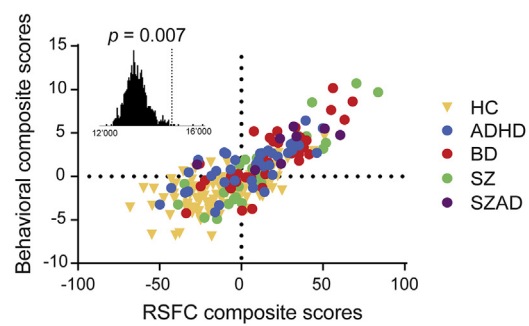
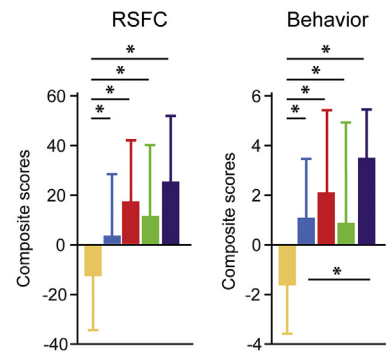
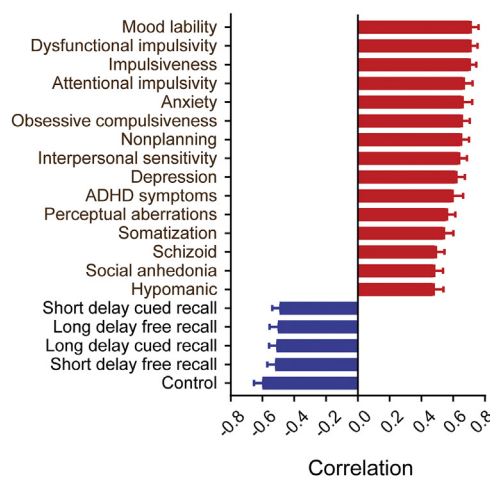
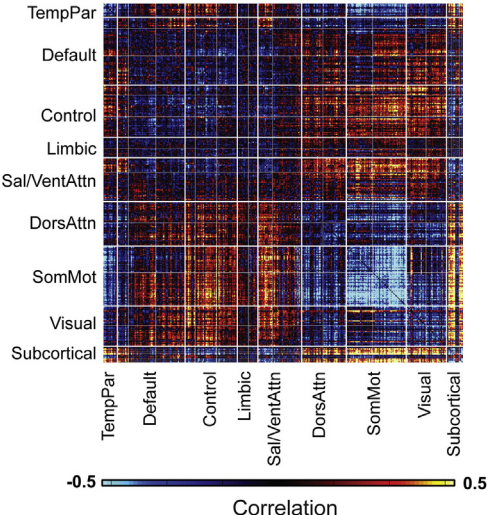
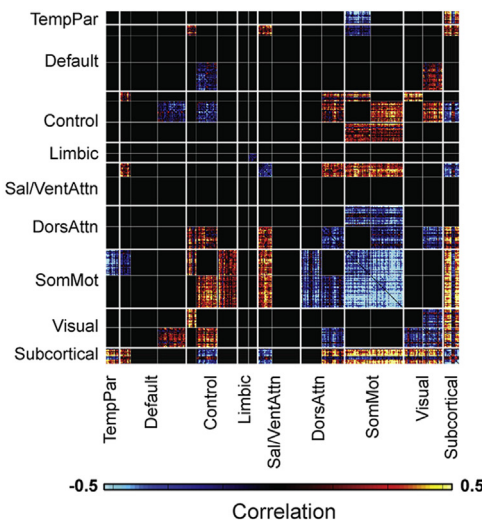
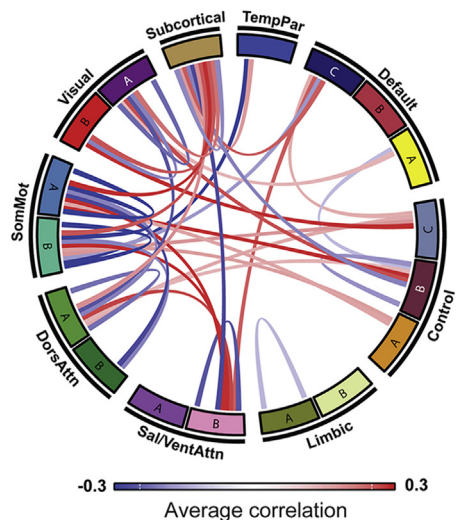


Figure 1. Brain parcellation. **(A)** Schaefer's 400 cortical regions (53). The parcels are assigned to 17 resting-state networks, which are further grouped into 8 major networks: default mode (Default A/B/C), executive control (Control A/B/C), somatomotor (SomMot A/B), visual (Visual A/B), limbic (Limbic A/B), salience/ventral attention (Sal/VentAttn A/B), dorsal attention (DorsAttn A/B), and temporoparietal (TempPar) (53). We note that the 400 cortical regions were not symmetric. **(B)** Nineteen subcortical regions (54). All subcortical regions, except the brainstem, are lateralized. The 419 regions of interest were used to compute 419×419 resting-state functional connectivity matrices for each participant. Because the resting-state functional connectivity matrices were symmetric, only the upper triangular portions of the matrices were considered in subsequent analyses (although full matrices are shown for visualization). DC, diencephalon.

LC1 - General psychopathology**A Correlation between composite scores****B Group differences in composite scores****C Behavioral loadings****D Unthresholded RSFC loadings****E Thresholded RSFC loadings****F Significant RSFC network loadings**

together with 1 volume before and 2 volumes after. Uncensored segments of data fewer than 5 contiguous volumes were also flagged as outliers (50). Scans with more than 50% outliers were removed completely. A total of 36 participants were excluded for excessive head motion, resulting in a final sample of 224 participants (110 HCs, 40 patients with BD, 37 patients with ADHD, 29 patients with SZ, 8 patients with SZAD).

We regressed out 18 nuisance regressors comprising 6 motion parameters, averaged ventricular signal, averaged white matter signal, global signal, and their temporal derivatives. Outlier volumes were ignored when computing the regression coefficients. The data were interpolated across censored frames using least squares spectral estimation (51). A bandpass filter ($0.009 \text{ Hz} \leq f \leq 0.08 \text{ Hz}$) was applied. Finally, the preprocessed fMRI data were projected onto the nonsymmetric FreeSurfer fsaverage6 surface space. Because global signal regression is controversial (52), we performed control analyses using an alternative strategy (see “Control and Reliability Analyses” section below).

Resting-State Functional Connectivity

RSFC (Pearson’s correlation) was computed among the average time series of 400 cortical (53) and 19 subcortical (54) regions of interest (ROIs) covering the entire brain (Figure 1), resulting in a 419×419 RSFC matrix for each participant. Because age, sex, education, site, and head motion (mean framewise displacement) were different across groups (Table 1), they were regressed from both behavioral and RSFC data.

Partial Least Squares

PLS is a multivariate data-driven statistical technique that maximizes the covariance between two matrices by deriving LCs, which are optimal linear combinations of the original matrices (55,56). We applied PLS to the RSFC and behavioral measures of all participants while ignoring diagnostic categories. Each LC is characterized by a distinct RSFC pattern (called RSFC saliences) and a distinct behavioral profile (called behavioral saliences). By linearly projecting the RSFC and behavioral measures of each participant onto their respective saliences, we obtain individual-specific RSFC and behavioral composite scores for each LC. By construction, PLS seeks to find saliences that maximize across-participant covariance between the RSFC and behavioral composite scores. The number of significant LCs was determined by a permutation test (1000 permutations). The p values

(from the permutation) for the top five LCs were corrected for multiple comparisons using a false discovery rate (FDR) of $q < .05$. See *Supplemental Methods* for details.

To interpret the LCs, we computed Pearson’s correlations between the original RSFC data and RSFC composite scores as well as between the original behavioral measures and behavioral composite scores for each LC (57,58). A large positive (or negative) correlation for a particular behavioral measure for a given LC indicates greater importance of the behavioral measure for the LC. Similarly, a large positive (or negative) correlation for a particular RSFC measure for a given LC indicates greater importance of the RSFC measure for the LC. To estimate confidence intervals for these correlations, we applied a bootstrapping procedure that generated 500 samples from subjects’ RSFC and behavioral data. Z scores were calculated by dividing each correlation coefficient by its bootstrap-estimated standard deviation. To limit the number of multiple comparisons, the bootstrapped correlations between the RSFC data and RSFC composite scores were averaged across ROI pairs within and between 18 networks (Figure 1), resulting in 18×18 correlation matrices, before computing bootstrapped Z scores. The Z scores were converted to p values and were FDR corrected ($q < .05$) along with other post hoc tests. Code for this work can be found here: https://github.com/ThomasYeoLab/CBIG/tree/master/stable_projects/disorder_subtypes/Kebets2019_TransdiagnosticComponents.

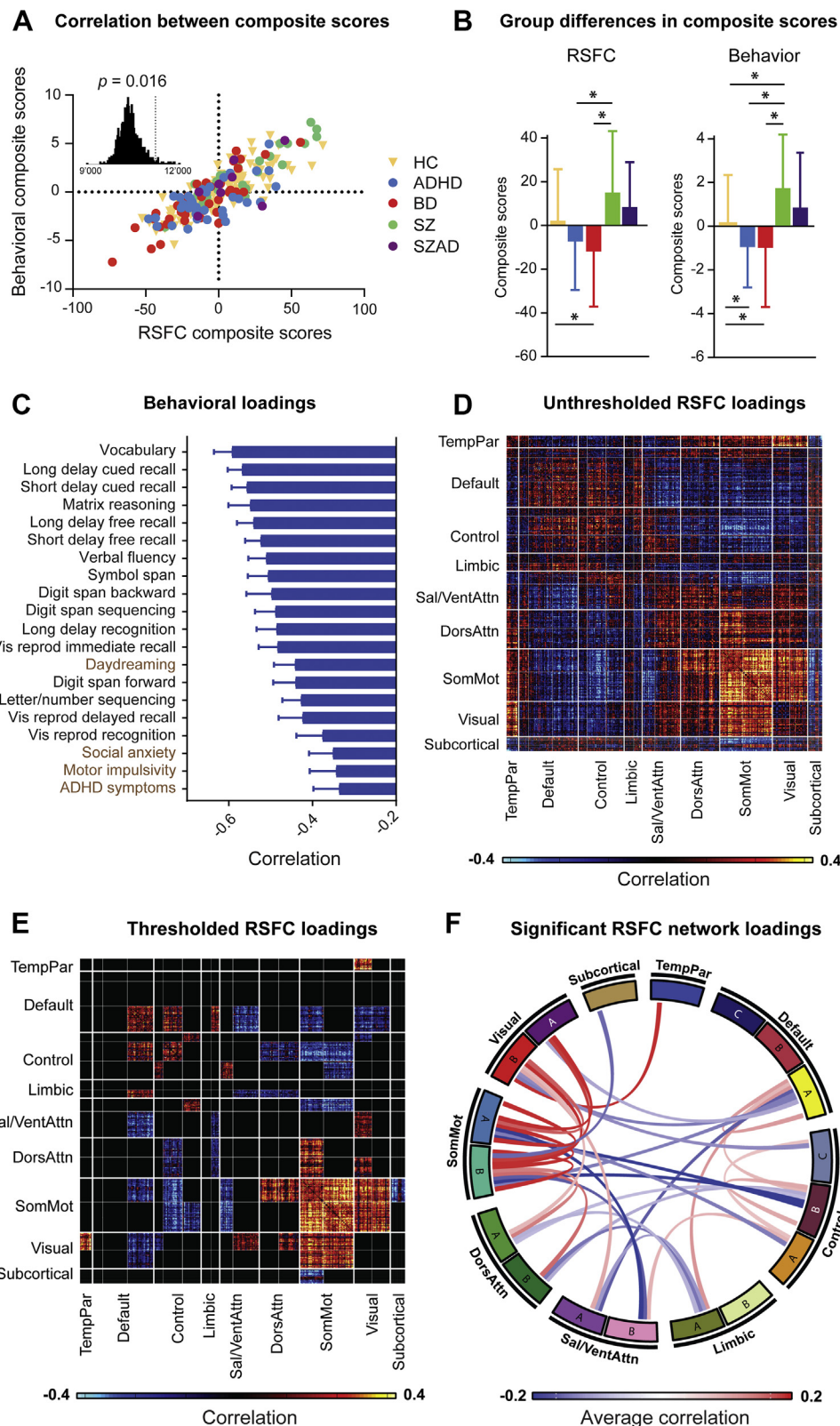
Post Hoc Analyses

Two-sample t tests were performed to test whether RSFC and behavioral composite scores for LCs 1, 2, and 3 were different between participants with different diagnoses, medication, and substance use. See *Supplemental Methods* for details.

We also tested whether the composite scores were associated with age, sex, years of education, acquisition site, head motion, and medication load. Pearson’s correlations were performed for continuous measures, and t tests were performed for binary measures. As control analyses, we applied generalized linear models with linear hypothesis tests to assess the impact of diagnosis (while controlling for medication and substance use), medication (while controlling for diagnosis and substance use), and substance use (while controlling for diagnosis and medication use). See *Supplemental Methods* for details.

All post hoc analyses used all participants, and FDR correction ($q < .05$) was applied to all post hoc tests.

Figure 2. First latent component (LC1) reflects general psychopathology. (A) Correlation between individual-specific resting-state functional connectivity (RSFC) and behavioral composite scores of participants. Scatterplots for each primary diagnostic group are found in *Supplemental Figure S9*. Inset shows null distribution obtained by permutation testing. Note that the null distribution is not centered at zero. The dashed line indicates the actual singular value obtained for LC1. (B) Group differences in RSFC and behavioral composite scores. Asterisks indicate t tests that survived false discovery rate correction ($q < .05$). Healthy control individuals (HC) had significantly lower RSFC and behavioral composite scores compared with all patient groups. Patients with attention-deficit/hyperactivity disorder (ADHD) also had significantly lower behavioral composite scores compared with patients with schizoaffective disorder (SZAD). (C) Top 20 strongest correlations between participants’ behavioral measures and their behavioral composite scores. Greater loading on LC1 was associated with higher measures of psychopathology and worse control. Error bars indicate bootstrapped standard deviation. Behavioral measures for which higher values indicate worse outcomes are colored brown. For example, anxiety is colored brown because higher values indicate worse anxiety. (D) Unthresholded correlations between participants’ RSFC data and their RSFC composite scores. Red (or blue) color indicates that greater RSFC is positively (or negatively) associated with LC1. (E) Thresholded correlations between participants’ RSFC data and their RSFC composite scores, whereby only within-network or between-network blocks with significant bootstrapped Z scores are shown (false discovery rate $q < .05$). (F) Correlations between participants’ RSFC data and their RSFC composite scores, averaged within and between networks with significant bootstrapped Z scores. BD, bipolar disorder; Control, executive control; Default, default mode; DorsAttn, dorsal attention; Sal/VentAttn, salience/ventral attention; SomMot, somatomotor; SZ, schizophrenia; TempPar, temporo-parietal.

LC2 - Cognitive dysfunction

Control and Reliability Analyses

Several analyses were performed to ensure robustness of the LCs ([Supplemental Methods](#)). First, we tested whether we could replicate the brain-behavior associations identified with rs-fMRI using task fMRI data. Second, we performed a 5-fold cross-validation of the PLS analysis. Third, we applied principal component analysis to the behavioral measures to test the robustness of our results. Fourth, we applied quantile normalization to improve the Gaussianity of the behavioral data distributions before PLS. Moreover, four behavioral measures were skewed, so PLS was recomputed after having removed these measures. Furthermore, some clinical measures might be too similar to diagnostic variables, so we recomputed PLS after removing measures that distinguished one diagnostic group from other groups. Fifth, instead of regressing age, sex, education, site, and motion from the data, these variables were added to the behavioral data for the PLS analysis. Sixth, we used CompCor ([59](#)) instead of global signal regression in the rs-fMRI preprocessing. Furthermore, to ensure that our results were not driven by the HCs or by case-control differences, PLS was recomputed using only control individuals or only patients. Finally, PLS was recomputed for participants of each site separately to ensure that results were not driven by a single site.

RESULTS

PLS Reveals Three Robust LCs Linking Behavior and Brain Function

We applied PLS to whole-brain RSFC and 54 behavioral measures of 224 participants across diagnostic categories. [Supplemental Figure S1](#) shows the amount of covariance explained by each LC. Four LCs survived permutation testing with FDR correction ($q < .05$) ([Figures 2A, 3A, and 4A](#) and [Supplemental Figure S2A](#)). Because the fourth LC ([Supplemental Figure S2](#)) was not robust to control analyses (see below), we focus on the first, second, and third LCs (LC1, LC2, and LC3, respectively) for the remainder of this article. We also note that none of the confounds (age, sex, education, site, or motion) examined in [Table 1](#) was associated with any component ([Supplemental Table S5](#)).

LC1 Reflects General Psychopathology

LC1 accounted for 20% of RSFC-behavior covariance ([Supplemental Figure S1](#)), with significant association ($r = .78$,

$p = .007$) between RSFC and behavioral composite scores ([Figure 2A](#)).

[Figure 2C](#) shows the top correlations between LC1's behavioral composite score and the 54 behavioral measures ([Supplemental Table S3](#) shows all behavioral measures, including those not included in the PLS analysis, e.g., clinical measures not administered to HCs). Greater behavioral composite score was associated with greater psychopathology (e.g., mood lability, dysfunctional impulsivity, anxiety) and worse control (which measures capacity to control one's behavior).

Correlations between LC1's RSFC composite scores and the RSFC data among 400 cortical and 19 subcortical ROIs ([Figure 1](#)) are shown in [Figure 2D](#) (unthresholded correlations) and [Figure 2E](#) (significant correlations). [Figure 2F](#) shows the significant RSFC correlations averaged within and between networks. Greater RSFC composite score was associated with decreased RSFC within the somatomotor networks. Sensory-motor (visual and somatomotor) and dorsal attention A networks showed greater RSFC with the salience B network and with subcortical regions (thalamus, ventral diencephalon, cerebellum, caudate, putamen, and pallidum).

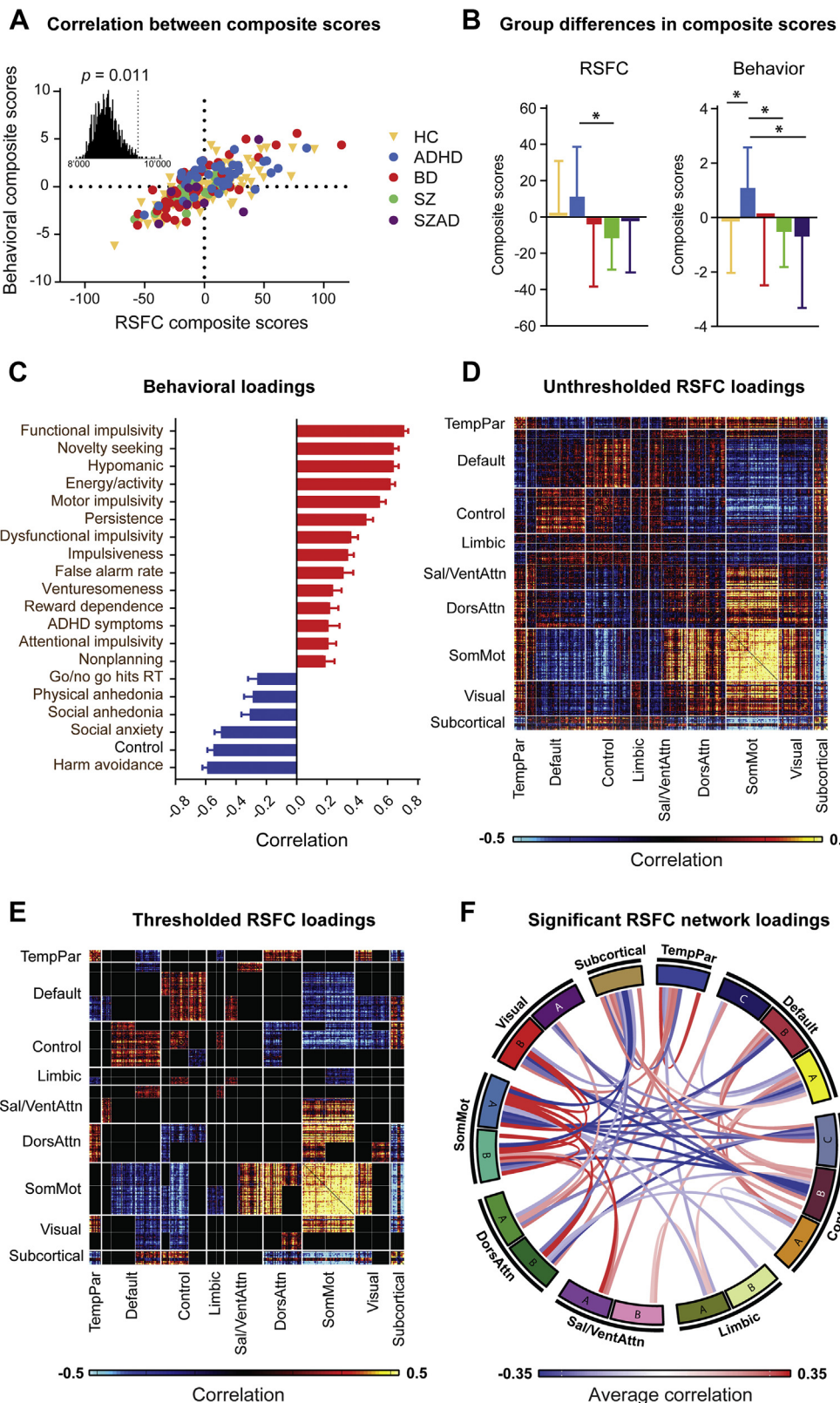
Consistent with the interpretation that LC1 reflects general psychopathology, both RSFC and behavioral composite scores were lower in HCs compared with all patient groups ([Figure 2B](#)) even after controlling for medication and substance use ([Supplemental Figure S3](#)). Additional results on medication and substance use are found in [Supplemental Table S5](#), [Supplemental Figures S4 to S7](#), and [Supplemental Results](#).

LC2 Reflects Differential Cognitive Impairment Between Disorders

LC2 accounted for 12% of RSFC-behavior covariance ([Supplemental Figure S1](#)), with significant association ($r = .83$, $p = .016$) between RSFC and behavioral composite scores ([Figure 3A](#)). Greater behavioral composite score was associated with worse cognitive performance in language, memory, and executive function but also with less social anxiety, motor impulsivity, and ADHD symptoms ([Figure 3C](#)).

Greater RSFC composite score was associated with increased RSFC within the somatomotor and default A networks and between the somatomotor and visual networks ([Figure 3D-F](#)). Somatomotor and attentional networks showed decreased RSFC with control B and salience B networks.

Figure 3. Second latent component (LC2) reflects cognitive dysfunction. **(A)** Correlation between individual-specific resting-state functional connectivity (RSFC) and behavioral composite scores of participants. Scatterplots for each primary diagnostic group are found in [Supplemental Figure S10](#). Inset shows null distribution obtained by permutation testing. Note that the null distribution is not centered at zero. The dashed line indicates the actual singular value obtained for LC2. **(B)** Group differences in RSFC and behavioral composite scores. Asterisks indicate t tests that survived false discovery rate correction ($q < .05$). Patients with schizophrenia (SZ) had significantly higher RSFC and behavioral composite scores compared with patients with attention-deficit/hyperactivity disorder (ADHD) and bipolar disorder (BD). Healthy control individuals (HC) also had higher RSFC composite scores than patients with BD, higher behavioral composite scores than patients with ADHD and BD, and lower behavioral composite scores than patients with SZ. **(C)** Top 20 strongest correlations between participants' behavioral measures and their behavioral composite scores. Greater loading on LC2 was associated with greater impairment across several cognitive domains (including language, memory, and executive functions) but also with less daydreaming, social anxiety, motor impulsivity, and ADHD symptoms. Error bars indicate bootstrapped standard deviations. Behavioral measures for which higher values indicate worse outcomes are colored brown. For example, ADHD symptoms is colored brown because higher values indicate more ADHD symptoms. **(D)** Unthresholded correlations between participants' RSFC data and their RSFC composite scores. Red (or blue) color indicates that greater RSFC is positively (or negatively) associated with LC2. **(E)** Thresholded correlations between participants' RSFC data and their RSFC composite scores, whereby only within-network or between-network blocks with significant bootstrapped Z scores are shown (false discovery rate $q < .05$). **(F)** Correlations between participants' RSFC data and their RSFC composite scores, averaged within and between networks with significant bootstrapped Z scores. Control, executive control; Default, default mode; DorsAttn, dorsal attention; Sal/VentAttn, salience/ventral attention; SomMot, somatomotor; SZAD, schizoaffective disorder; TempPar, tempoparietal; Vis reprod, visual reproduction.

LC3 - Impulsivity

RSFC and behavioral composite scores were higher in patients with SZ or SZAD than in patients with ADHD or BD, although this was significant only with respect to patients with SZ (potentially because of the small number of SZAD participants) (Figure 3B). Differences remained significant after controlling for medication and substance use (Supplemental Figure S3). Additional results on medication and substance use are found in Supplemental Table S5, Supplemental Figures S4 to S5, and Supplemental Results.

LC3 Reflects Greater Impulsivity

LC3 accounted for 8% of RSFC-behavior covariance (Supplemental Figure S1), with significant association ($r = .73$, $p = .011$) between RSFC and behavioral composite scores (Figure 4A). Figure 4C shows that greater behavioral composite score was associated with greater impulsivity (e.g., functional and motor impulsivity, novelty seeking) as well as lower control, harm avoidance, and social anxiety.

Greater RSFC composite score was associated with increased RSFC within the somatomotor networks (Figure 4D–F). Somatomotor networks also showed greater RSFC with visual B, dorsal attention B, and salience A networks and showed lower RSFC with default A and B networks, control B network, and subcortical regions (caudate, cerebellum, and thalamus). Finally, RSFC was also increased between default (A and B) and control networks.

Patients with ADHD had higher RSFC and behavior composite scores than patients with SZ and had higher behavioral composite scores than HCs (Figure 4B). However, only the difference between patients with ADHD and HCs was significant after controlling for medication and substance use (Supplemental Figure S3). Additional results on medication and substance use are found in Supplemental Table S5, Supplemental Figures S4 to S7, and Supplemental Results.

Somatomotor Networks Are Transdiagnostic Hubs

Supplemental Figure S8 shows functional connections unique to each LC obtained by comparing Figures 2E, 3E, and 4E. Supplemental Table S6 summarizes behavioral measures that are unique to each LC, or that load on multiple LCs, obtained by comparing Figures 2C, 3C, and 4C.

To examine functional connections common across LCs, within-network and between-network blocks with significant bootstrapped Z scores (Figures 2F, 3F, and 4F) were binarized

and summed across the first three LCs (Figure 5A). Absolute correlations within blocks that were significant in all three LCs (Figures 2E, 3E, and 4E) were summed across the LCs to obtain the magnitude of correlations common across the LCs (Figure 5B). Somatomotor networks' connections appeared prominently, including connections within the somatomotor networks as well as somatomotor networks' connections with control B, dorsal attention B, and subcortical regions (caudate, putamen, thalamus, and cerebellum). Finally, Figure 5C shows the strength of involvement of each ROI obtained by summing the rows of Figure 5B.

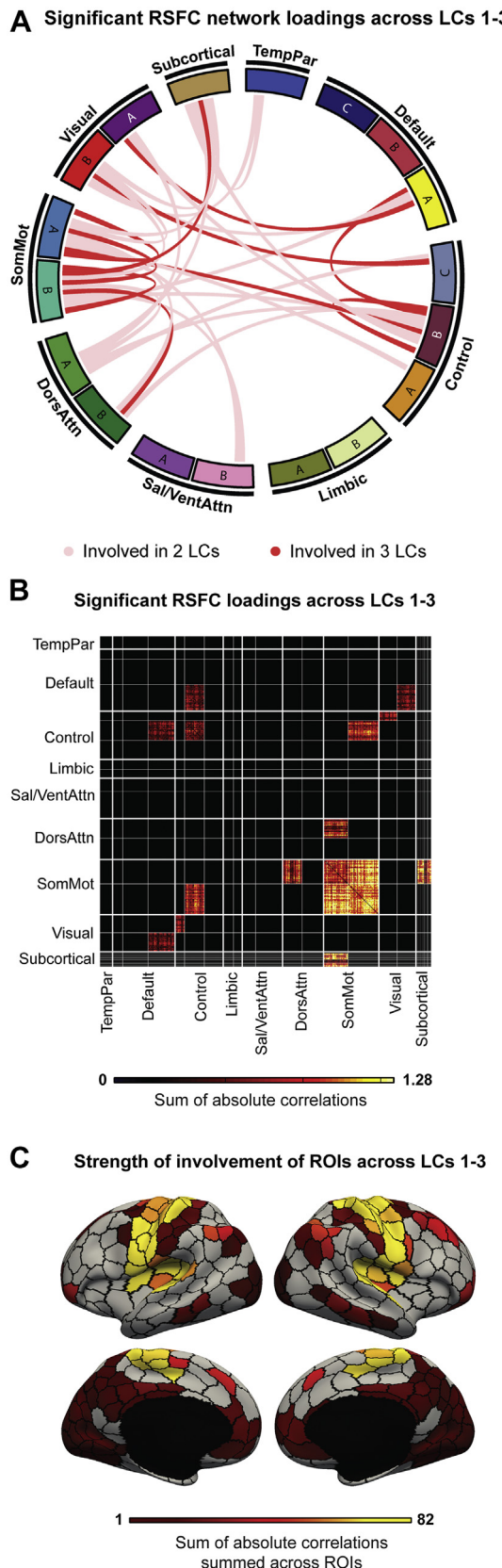
Control and Reliability Analyses

We summarize several analyses that ensured robustness of the LCs. See Supplemental Results and Supplemental Tables S8 to S10 for details. First, PLS components estimated from RSFC successfully generalized to task functional connectivity in the same participants. Second, 5-fold cross-validation was successful; PLS components estimated from 80% of the participants successfully generalized to the remaining 20% of participants. Third, the top three principal components of the behavioral measures were highly correlated to the behavioral saliences of LCs 1, 2, and 3 ($r \geq .97$), suggesting robustness across analytic approaches. Fourth, PLS components were robust to non-Gaussian and skewed behavioral distributions and were not driven by diagnostic variables. Fifth, instead of regressing age, sex, education, site, and motion from the data, these variables were added to the behavioral data for the PLS analysis. The results were largely unchanged. Sixth, we used CompCor (59) instead of global signal regression in the rs-fMRI preprocessing. The first three LCs were largely unchanged, but not the fourth LC. Hence, we focused on LCs 1, 2, and 3 in this article. To ensure that our results were not driven by the large number of HCs or by case-control group differences, PLS was recomputed using only controls or only patients. In both models, we found moderate to high correlations with original saliences. Finally, we recomputed PLS within each site and found moderate to high correlations with the original saliences.

DISCUSSION

We identified three LCs representing general psychopathology, cognitive dysfunction, and impulsivity, which were associated with distinct whole-brain RSFC patterns across mental

Figure 4. Third latent component (LC3) reflects impulsivity. (A) Correlation between individual-specific resting-state functional connectivity (RSFC) and behavioral composite scores of participants. Scatterplots for each primary diagnostic group are found in Supplemental Figure S11. Inset shows null distribution obtained by permutation testing. Note that the null distribution is not centered at zero. The dashed line indicates the actual singular value obtained for LC3. (B) Group differences in RSFC and behavioral composite scores. Asterisks indicate t tests that survived false discovery rate correction ($q < .05$). Patients with attention-deficit/hyperactivity disorder (ADHD) had significantly higher RSFC and behavioral composite scores compared with patients with schizophrenia (SZ). Patients with ADHD also had significantly higher behavioral composite scores compared with healthy control individuals (HC) and patients with schizoaffective disorder (SZAD). (C) Top 20 strongest correlations between participants' behavioral measures and their behavioral composite scores. Great loading on LC3 was positively associated with several measures of impulsivity and was negatively associated with harm avoidance and control. Error bars indicate bootstrapped standard deviations. Behavioral measures for which higher values indicated worse outcomes are colored brown. For example, false alarm rate is colored brown because higher values indicated greater false alarm rate. (D) Unthresholded correlations between participants' RSFC data and their RSFC composite scores, showing the connections that contribute most to LC3. Red (or blue) color indicates that greater RSFC is positively (or negatively) associated with LC3. (E) Thresholded correlations between participants' RSFC data and their RSFC composite scores, whereby only within-network or between-network blocks with significant bootstrapped Z scores are shown (false discovery rate $q < .05$). (F) Correlations between participants' RSFC data and their RSFC composite scores, averaged within and between networks with significant bootstrapped Z scores. BD, bipolar disorder; Control, executive control; Default, default mode; DorsAttn, dorsal attention; RT, reaction time; Sal/VentAttn, salience/ventral attention; SomMot, somatomotor; TempPar, temporoparietal.



health and disease. All three components implicated connectivity of the somatomotor network with subcortical and cortical executive networks. These brain-behavior associations might index intermediate neurobiological processes and potentially serve as transdiagnostic phenotypes, providing a more comprehensive characterization of individuals' phenotypic variability.

Somatomotor Networks Are Transdiagnostic Hubs

The implication of the somatomotor network across multiple dimensions might seem surprising. However, closer inspection of previous case-control neuroimaging studies suggests that the somatomotor regions are often reported, but not emphasized, within prevailing psychiatric models. For example, altered RSFC within the somatomotor network (21,25,60–62), as well as between the somatomotor networks and thalamus (60,63–69), have been documented in case-control studies investigating SZ, SZAD, and BD. Altered thalamo-somatomotor RSFC has also been linked to SZ symptom severity (60,63,64). One recent study found RSFC involving somatosensory, motor, basal ganglia, thalamic, and visual regions to be associated with the p factor (12). Our results extend previous work by showing that dysconnectivity patterns of these regions are linked to variation in three domains: general psychopathology, cognitive dysfunction, and impulsivity.

In addition to dysconnectivity of the somatomotor network, sensory processing has been found to be disturbed in SZ (70) and BD (71,72). Moreover, the diagnostic criteria for BD and ADHD include motor features (73,74). Indeed, motor dysfunction has been documented in many psychiatric disorders (75), preceding disease onset and predicting disease progression (76–78). Because all three LCs in this study featured connectivity between somatomotor and executive networks, these sensory-motor deficits might arise from impaired top-down control over lower-level processes. Another possible mechanism is impaired ability to decode information coming from sensory regions, whereby lower-level sensory deficits may cascade up the system, undermining higher-order cognitive functions (70). Overall, our findings suggest that sensory-motor processes affect symptomatology, cognitive function, and personality. Investigating these processes in the future may therefore inform the underlying etiology of various aspects of psychopathology.

Figure 5. Functional connections involved in multiple latent components (LCs). **(A)** Within-network and between-network blocks with significant bootstrapped Z scores (Figures 2F, 3F, and 4F) were binarized and summed across the first three LCs. Within-network and between-network blocks that were significant in only one LC were changed to zero. **(B)** Sum of absolute correlations within significant within-network and between-network blocks (Figures 2E, 3E, and 4E). Connections involving the somatosensory-motor (somatomotor) networks were involved in all three LCs. Furthermore, even though we did not focus on the fourth LC in this study, somatomotor networks' connections also featured prominently in the fourth LC (Supplemental Figure S2D-F). **(C)** Strength of involvement of each region of interest (ROI) was obtained by summing the rows of panel B and displaying on a surface map. The strength of involvement of the top 50 ROIs can be found in Supplemental Table S7. Control, executive control; Default, default mode; DorsAttn, dorsal attention; RSFC, resting-state functional connectivity; Sal/VentAttn, salience/ventral attention; SomMot, somatomotor; TempPar, temporoparietal.

Relations to Other Transdiagnostic Studies

LC1 appeared to reflect the *p* factor widely discussed in transdiagnostic cohorts (10–15). On the other hand, LC2 (cognitive dysfunction) and LC3 (impulsivity) have been featured less frequently and provided further insights into heterogeneity among individuals.

LC2 captured dysfunction across multiple cognitive domains. Interestingly, HCs had almost no loadings on LC2, which argues against LC2 representing general intelligence. Instead, LC2 was largely driven by greater cognitive impairment in patients with SZ or SZAD compared with HCs and patients with ADHD or BD. This is consistent with previous studies showing more severe deficits in patients with SZ or SZAD compared with other psychiatric groups such as patients with BD (3,79–82). However, LC2 was not purely cognitive given that it was also driven by worse symptoms in individuals with ADHD or BD compared to individuals with SZ or HCs.

Although central to several psychiatric conditions [e.g., ADHD, substance disorder (83)], impulsivity factors have been reported in only one recent transdiagnostic study but were not associated with any RSFC pattern (12). In our case, the impulsivity measures driving LC3 indexed response inhibition (e.g., false alarm rate), novelty seeking, and hyperactivity (e.g., energy/activity). This component differentiated patients with ADHD from HCs, consistent with hyperactivity/impulsivity being characteristic of ADHD (73).

Strengths and Limitations

One strength of our study is the use of a whole-brain data-driven approach and a broad set of behavioral measures. The components we identified with RSFC generalized well to task fMRI data and were robust across alternative methodological strategies. Nonetheless, our work has several limitations. First, the sample size of each patient group was small. This was not an issue for the PLS analysis because diagnostic categories were not used. However, the limited sample sizes do affect post hoc analyses, for example, when comparing the SZAD group with other patient groups. Future research involving larger samples and more diagnostic categories is warranted. Second, most scales measuring symptom severity were administered only to patients, which limited the number of clinical measures that could be used [cf. (17)]. Moreover, while the cortex was parcellated into functionally defined regions, the subcortical regions were more coarsely delineated based on macroanatomy. A finer parcellation might better capture cortical-subcortical associations. Field maps were not collected, so distortion correction was not performed. Furthermore, PLS covariances should not be interpreted as actual effect sizes, as can be seen by the fact that the null distributions of singular values were not centered at zero (insets in Figures 2A, 3A, and 4A). Indeed, cross-validated correlations (which are more appropriate measures of the effect size), while statistically significant, were much lower than PLS correlations (Supplemental Table S8). Finally, our results might be affected by the particular combination of psychiatric disorders and behavioral measures available in this dataset. Future studies will benefit from the increasing availability of broad phenotypic batteries that assess multiple domains of behavior, cognition, and genetics (84,85).

Conclusions

By identifying three components that characterized individuals' variability in psychopathology, cognitive impairment, and impulsivity, our work has allowed highlighting the multi-faceted role of somatomotor regions along these dimensions. Our study thus adds further evidence to the benefits of including a broad range of behavioral measures to capture brain-behavior associations across psychiatric boundaries. Identifying such transdiagnostic associations might help to uncover common neurobiological mechanisms and explain high comorbidity rates in psychiatry. Code for this work can be found here: https://github.com/ThomasYeoLab/CBIG/tree/master/stable_projects/disorder_subtypes/Kebets2019_TransdiagnosticComponents.

ACKNOWLEDGMENTS AND DISCLOSURES

This work was supported by Singapore Ministry of Education Tier 2 (Grant No. MOE2014-T2-2-016 [to BTTY]), National University of Singapore (NUS) Strategic Research (Grant No. DPRT/944/09/14 [to BTTY]), NUS School of Medicine Aspiration Fund (Grant No. R185000271720 [to BTTY]), Singapore National Medical Research Council (Grant No. CBRG/0088/2015 [to BTTY]), NUS Young Investigator Award, and the Singapore National Research Foundation Fellowship (Class of 2017). Our research also used resources provided by the Center for Functional Neuroimaging Technologies (Grant No. P41EB015896 [to BTTY]) and instruments supported by Grant Nos. 1S10RR023401, 1S10RR019307, and 1S10RR023043 from the Athinoula A. Martinos Center for Biomedical Imaging at Massachusetts General Hospital. Our computational work was partially performed on resources of the National Supercomputing Centre, Singapore (<https://www.nscc.sg>).

We thank the investigators Robert Bilder, Russell Poldrack, Tyrone Cannon, Edythe London, Nelson Freimer, Eliza Congdon, Katherine Karlsgodt, and Fred Sabb for sharing their data publicly.

A previous version of this article was published as a preprint on bioRxiv. All data are publicly available via the OpenfMRI database (<https://openfmri.org/dataset>). The accession number of this dataset is ds000030.

The authors report no biomedical financial interests or potential conflicts of interest.

ARTICLE INFORMATION

From the Department of Electrical and Computer Engineering (VK, CO, ST, JL, NS, RK, BTTY), Clinical Imaging Research Centre, N.I Institute for Health and Memory Networks Program, National University of Singapore, Singapore; Graduate School for Integrative Sciences and Engineering (BTTY), National University of Singapore, Singapore; and Centre for Cognitive Neuroscience (BTTY), Duke-NUS Medical School, Singapore; Department of Radiology and Medical Informatics (VK), University of Geneva, Geneva, Switzerland; Neuropsychopharmacology Unit (CO), Centre for Psychiatry, Imperial College London, London, United Kingdom; Department of Psychology (AJH) and Department of Psychiatry (AJH), Yale University, New Haven, Connecticut; Athinoula A. Martinos Center for Biomedical Imaging (AJH, BTTY), Massachusetts General Hospital, Charlestown, and Department of Psychiatry (AJH), Massachusetts General Hospital, Boston, Massachusetts; and Department of Psychology (RAP) and Department of Electrical Engineering (ST), Stanford University, Stanford, California.

Address correspondence to B.T. Thomas Yeo, Ph.D., Department of Electrical and Computer Engineering, Block E4, Level 5, Room 42, National University of Singapore, 4 Engineering Drive 3, Singapore 117583; E-mail: thomas.yeo@nus.edu.sg.

Received Nov 19, 2018; revised May 15, 2019; accepted Jun 5, 2019.
Supplementary material cited in this article is available online at <https://doi.org/10.1016/j.biopsych.2019.06.013>.

REFERENCES

1. Russo M, Levine SZ, Demjaha A, Di Forti M, Bonaccorso S, Fearon P, et al. (2014): Association between symptom dimensions and categorical diagnoses of psychosis: A cross-sectional and longitudinal investigation. *Schizophr Bull* 40:111–119.
2. Tamminga CA, Ivleva EI, Keshavan MS, Pearlson GD, Clementz BA, Witte B, et al. (2013): Clinical phenotypes of psychosis in the Bipolar-Schizophrenia Network on Intermediate Phenotypes (B-SNIP). *Am J Psychiatry* 170:1263–1274.
3. Stefanopoulou E, Manoharan A, Landau S, Geddes JR, Goodwin G, Frangou S (2009): Cognitive functioning in patients with affective disorders and schizophrenia: A meta-analysis. *Int Rev Psychiatry* 21:336–356.
4. Pettersson E, Larsson H, Lichtenstein P (2016): Common psychiatric disorders share the same genetic origin: A multivariate sibling study of the Swedish population. *Mol Psychiatry* 21:717–721.
5. Kessler RC, Ormel J, Petukhova M, McLaughlin KA, Green JG, Russo LJ, et al. (2011): Development of lifetime comorbidity in the World Health Organization world mental health surveys. *Arch Gen Psychiatry* 68:90–100.
6. Insel T, Cuthbert B, Garvey M, Heinssen R, Pine DS, Quinn K, et al. (2010): Research domain criteria (RDoC): Toward a new classification framework for research on mental disorders. *Am J Psychiatry* 167:748–751.
7. Cuthbert BN (2014): The RDoC framework: Facilitating transition from ICD/DSM to dimensional approaches that integrate neuroscience and psychopathology. *World Psychiatry* 13:28–35.
8. Kotov R, Krueger RF, Watson D, Achenbach TM, Althoff RR, Bagby RM, et al. (2017): The hierarchical taxonomy of psychopathology (HiTOP): A dimensional alternative to traditional nosologies. *J Abnorm Psychol* 126:454–477.
9. Kotov R, Krueger RF, Watson D (2018): A paradigm shift in psychiatric classification: The hierarchical taxonomy of psychopathology (HiTOP). *World Psychiatry* 17:24–25.
10. Shanmugan S, Wolf DH, Calkins ME, Moore TM, Ruparel K, Hopson RD, et al. (2016): Common and dissociable mechanisms of executive system dysfunction across psychiatric disorders in youth. *Am J Psychiatry* 173:517–526.
11. Kaczkurkin AN, Moore TM, Calkins ME, Cricic R, Detre JA, Elliott MA, et al. (2018): Common and dissociable regional cerebral blood flow differences associate with dimensions of psychopathology across categorical diagnoses. *Mol Psychiatry* 23:1981–1989.
12. Van Dam NT, O'Connor D, Marcelli ET, Ho EJ, Cameron Craddock R, Tobe RH, et al. (2017): Data-driven phenotypic categorization for neurobiological analyses: Beyond DSM-5 labels. *Biol Psychiatry* 81:484–494.
13. Alnæs D, Kaufmann T, Doan NT, Córdova-Palomera A, Wang Y, Bettella F, et al. (2018): Association of heritable cognitive ability and psychopathology with white matter properties in children and adolescents. *JAMA Psychiatry* 75:287–295.
14. Elliott ML, Romer A, Knodt AR, Hariri AR (2018): A connectome-wide functional signature of transdiagnostic risk for mental illness. *Biol Psychiatry* 84:452–459.
15. Romer AL, Knodt AR, Houts R, Brigidi BD, Moffitt TE, Caspi A, et al. (2018): Structural alterations within cerebellar circuitry are associated with general liability for common mental disorders. *Mol Psychiatry* 23:1084–1090.
16. Caspi A, Houts RM, Belsky DW, Goldman-Mellor SJ, Harrington H, Israel S, et al. (2014): The ρ factor: One general psychopathology factor in the structure of psychiatric disorders? *Clin Psychol Sci* 2:119–137.
17. Xia CH, Ma Z, Cricic R, Gu S, Betzel RF, Kaczkurkin AN, et al. (2018): Linked dimensions of psychopathology and connectivity in functional brain networks. *Nat Commun* 9:3003.
18. Lahey BB, Krueger RF, Rathouz PJ, Waldman ID, Zald DH (2017): A hierarchical causal taxonomy of psychopathology across the life span. *Psychol Bull* 143:142–186.
19. Buckner RL, Krienen FM, Yeo BTT (2013): Opportunities and limitations of intrinsic functional connectivity MRI. *Nat Neurosci* 16:832–837.
20. Menon V (2011): Large-scale brain networks and psychopathology: A unifying triple network model. *Trends Cogn Sci* 15:483–506.
21. Baker JT, Holmes AJ, Masters GA, Yeo BTT, Krienen F, Buckner RL, et al. (2014): Disruption of cortical association networks in schizophrenia and psychotic bipolar disorder. *JAMA Psychiatry* 71:109–118.
22. Goodkind M, Eickhoff SB, Oathes DJ, Jiang Y, Chang A, Jones-Hagata LB, et al. (2015): Identification of a common neurobiological substrate for mental illness. *JAMA Psychiatry* 72:305–315.
23. Reinen JM, Chén OY, Hutchison RM, Yeo BTT, Anderson KM, Sabuncu MR, et al. (2018): The human cortex possesses a reconfigurable dynamic network architecture that is disrupted in psychosis. *Nat Commun* 9:1157.
24. Sprooten E, Rasgon A, Goodman M, Carlin A, Leibl E, Lee WH, et al. (2017): Addressing reverse inference in psychiatric neuroimaging: Meta-analyses of task-related brain activation in common mental disorders. *Hum Brain Mapp* 38:1846–1864.
25. Baker JT, Dillon DG, Patrick LM, Roffman JL, Brady RO, Pizzagalli DA, et al. (2019): Functional connectomics of affective and psychotic pathology. *Proc Natl Acad Sci U S A* 116:9050–9059.
26. Kernbach JM, Satterthwaite TD, Bassett DS, Smallwood J, Margulies D, Krall S, et al. (2018): Shared endo-phenotypes of default mode dysfunction in attention deficit/hyperactivity disorder and autism spectrum disorder. *Transl Psychiatry* 8:133.
27. Whitfield-Gabrieli S, Ford JM (2012): Default mode network activity and connectivity in psychopathology. *Annu Rev Clin Psychol* 8:49–76.
28. Holmes AJ, Patrick LM (2018): The myth of optimality in clinical neuroscience. *Trends Cogn Sci* 22:241–257.
29. Smith SM, Nichols TE, Vidaurre D, Winkler AM, Behrens TEJ, Glasser MF, et al. (2015): A positive-negative mode of population covariation links brain connectivity, demographics and behavior. *Nat Neurosci* 18:1565–1567.
30. Yeo BTT, Krienen FM, Eickhoff SB, Yaakub SN, Fox PT, Buckner RL, et al. (2015): Functional specialization and flexibility in human association cortex. *Cereb Cortex* 25:3654–3672.
31. Poldrack RA, Congdon E, Triplett W, Gorgolewski KJ, Karlsgodt KH, Mumford JA, et al. (2016): A genome-wide examination of neural and cognitive function. *Sci Data* 3:160110.
32. Drysdale AT, Grosenick L, Downar J, Dunlop K, Mansouri F, Meng Y, et al. (2017): Resting-state connectivity biomarkers define neurophysiological subtypes of depression. *Nat Med* 23:28–38.
33. Poldrack RA, Gorgolewski KJ (2017): OpenfMRI: Open sharing of task fMRI data. *NeuroImage* 144(pt B):259–261.
34. Bilder RM, Sabb FW, Cannon TD, London ED, Jentsch JD, Parker DS, et al. (2009): Phenomics: The systematic study of phenotypes on a genome-wide scale. *Neuroscience* 164:30–42.
35. First MB, Spitzer RL, Gibbon M, Williams JBW (2002): Structured Clinical Interview for DSM-IV-TR Axis I Disorders, Research Version, Patient Edition (SCID-I/P). New York: Biometrics Research, New York State Psychiatric Institute.
36. Gorgolewski KJ, Durnez J, Poldrack RA (2017): Preprocessed Consortium for Neuropsychiatric Phenomics dataset. F1000Research 6:1262.
37. Kong R, Li J, Orban C, Sabuncu MR, Liu H, Schaefer A, et al. (2019): Spatial topography of individual-specific cortical networks predicts human cognition, personality, and emotion. *Cereb Cortex* 29:2533–2551.
38. Li J, Kong R, Liégeois R, Orban C, Tan Y, Sun N, et al. (2019): Global signal regression strengthens association between resting-state functional connectivity and behavior. *NeuroImage* 196:126–141.
39. Dale AM, Fischl B, Sereno MI (1999): Cortical surface-based analysis: I. Segmentation and surface reconstruction. *NeuroImage* 9:179–194.
40. Fischl B, Liu A, Dale AM (2001): Automated manifold surgery: Constructing geometrically accurate and topologically correct models of the human cerebral cortex. *IEEE Trans Med Imaging* 20:70–80.
41. Ségonne F, Pacheco J, Fischl B (2007): Geometrically accurate topology-correction of cortical surfaces using nonseparating loops. *IEEE Trans Med Imaging* 26:518–529.
42. Fischl B (2012): FreeSurfer. *NeuroImage* 62:774–781.
43. Fischl B, Sereno MI, Dale AM (1999): Cortical surface-based analysis: II. Inflation, flattening, and a surface-based coordinate system. *NeuroImage* 9:195–207.

44. Fischl B, Sereno MI, Tootell RB, Dale AM (1999): High-resolution intersubject averaging and a coordinate system for the cortical surface. *Hum Brain Mapp* 8:272–284.
45. Jenkinson M, Beckmann CF, Behrens TEJ, Woolrich MW, Smith SM (2012): FSL. *Neuroimage* 62:782–790.
46. Smith SM, Jenkinson M, Woolrich MW, Beckmann CF, Behrens TEJ, Johansen-Berg H, et al. (2004): Advances in functional and structural MR image analysis and implementation as FSL. *Neuroimage* 23(suppl 1):S208–S219.
47. Greve DN, Fischl B (2009): Accurate and robust brain image alignment using boundary-based registration. *Neuroimage* 48:63–72.
48. Jenkinson M, Bannister P, Brady M, Smith S (2002): Improved optimization for the robust and accurate linear registration and motion correction of brain images. *Neuroimage* 17:825–841.
49. Power JD, Barnes KA, Snyder AZ, Schlaggar BL, Petersen SE (2012): Spurious but systematic correlations in functional connectivity MRI networks arise from subject motion. *Neuroimage* 59:2142–2154.
50. Gordon EM, Laumann TO, Adeyemo B, Huckins JF, Kelley WM, Petersen SE (2016): Generation and evaluation of a cortical area parcellation from resting-state correlations. *Cereb Cortex* 26:288–303.
51. Power JD, Mitra A, Laumann TO, Snyder AZ, Schlaggar BL, Petersen SE (2014): Methods to detect, characterize, and remove motion artifact in resting state fMRI. *Neuroimage* 84:320–341.
52. Murphy K, Fox MD (2017): Towards a consensus regarding global signal regression for resting state functional connectivity MRI. *Neuroimage* 154:169–173.
53. Schaefer A, Kong R, Gordon EM, Laumann TO, Zuo X-N, Holmes AJ, et al. (2018): Local-global parcellation of the human cerebral cortex from intrinsic functional connectivity MRI. *Cereb Cortex* 28:3095–3114.
54. Fischl B, Salat DH, Busa E, Albert M, Dieterich M, Haselgrove C, et al. (2002): Whole brain segmentation: Automated labeling of neuroanatomical structures in the human brain. *Neuron* 33:341–355.
55. McIntosh AR, Lobaugh NJ (2004): Partial least squares analysis of neuroimaging data: Applications and advances. *Neuroimage* 23(suppl 1):S250–S263.
56. McIntosh AR, Mišić B (2013): Multivariate statistical analyses for neuroimaging data. *Annu Rev Psychol* 64:499–525.
57. Courville T, Thompson B (2001): Use of structure coefficients in published multiple regression articles: β is not enough. *Educ Psychol Meas* 61:229–248.
58. Henson RK (2002): The logic and interpretation of structure coefficients in multivariate general linear model analyses. Presented at the Annual Meeting of the American Educational Research Association, New Orleans, LA, April 1–5.
59. Behzadi Y, Restom K, Liu J, Liu TT (2007): A component based noise correction method (CompCor) for BOLD and perfusion based fMRI. *Neuroimage* 37:90–101.
60. Bernard JA, Goen JRM, Maldonado T (2017): A case for motor network contributions to schizophrenia symptoms: Evidence from resting-state connectivity. *Hum Brain Mapp* 38:4535–4545.
61. Doucet GE, Bassett DS, Yao N, Glahn DC, Frangou S (2017): The role of intrinsic brain functional connectivity in vulnerability and resilience to bipolar disorder. *Am J Psychiatry* 174:1214–1222.
62. Kaufmann T, Skåtun KC, Alnæs D, Doan NT, Duff EP, Tønnesen S, et al. (2015): Disintegration of sensorimotor brain networks in schizophrenia. *Schizophr Bull* 41:1326–1335.
63. Anticevic A, Cole MW, Repovs G, Murray JD, Brumbaugh MS, Winkler AM, et al. (2014): Characterizing thalamo-cortical disturbances in schizophrenia and bipolar illness. *Cereb Cortex* 24:3116–3130.
64. Cheng W, Palaniyappan L, Li M, Kendrick KM, Zhang J, Luo Q, et al. (2015): Voxel-based, brain-wide association study of aberrant functional connectivity in schizophrenia implicates thalamocortical circuitry. *NPJ Schizophr* 1:15016.
65. Klingner CM, Langbein K, Dietzek M, Smesny S, Witte OW, Sauer H, et al. (2014): Thalamocortical connectivity during resting state in schizophrenia. *Eur Arch Psychiatry Clin Neurosci* 264:111–119.
66. Skåtun KC, Kaufmann T, Brandt CL, Doan NT, Alnæs D, Tønnesen S, et al. (2018): Thalamo-cortical functional connectivity in schizophrenia and bipolar disorder. *Brain Imaging Behav* 12:640–652.
67. Walther S, Stegmayer K, Federspiel A, Bohlhalter S, Wiest R, Viher PV (2017): Aberrant hyperconnectivity in the motor system at rest is linked to motor abnormalities in schizophrenia spectrum disorders. *Schizophr Bull* 43:982–992.
68. Woodward ND, Karbasforoushan H, Heckers S (2012): Thalamocortical dysconnectivity in schizophrenia. *Am J Psychiatry* 169:1092–1099.
69. Woodward ND, Heckers S (2016): Mapping thalamocortical functional connectivity in chronic and early stages of psychotic disorders. *Biol Psychiatry* 79:1016–1025.
70. Javitt DC, Freedman R (2015): Sensory processing dysfunction in the personal experience and neuronal machinery of schizophrenia. *Am J Psychiatry* 172:17–31.
71. Mrad A, Wassim Krir M, Ajmi I, Gaha L, Mechri A (2016): Neurological soft signs in euthymic bipolar I patients: A comparative study with healthy siblings and controls. *Psychiatry Res* 236:173–178.
72. Giakouraki SG, Rousos P, Rogdaki M, Karli C, Bitsios P, Frangou S (2007): Evidence of disrupted prepulse inhibition in unaffected siblings of bipolar disorder patients. *Biol Psychiatry* 62:1418–1422.
73. American Psychiatric Association (2013): Diagnostic and Statistical Manual of Mental Disorders, 5th ed. Arlington, VA: American Psychiatric Association.
74. American Psychiatric Association (2000): Diagnostic and Statistical Manual of Mental Disorders, 4th ed., text revision. Arlington, VA: American Psychiatric Association.
75. Bernard JA, Mittal VA (2015): Updating the research domain criteria: The utility of a motor dimension. *Psychol Med* 45:2685–2689.
76. Dean DJ, Kent JS, Bernard JA, Orr JM, Gupta T, Pelletier-Baldelli A, et al. (2015): Increased postural sway predicts negative symptom progression in youth at ultrahigh risk for psychosis. *Schizophr Res* 162:86–89.
77. Mittal VA, Walker EF, Bearden CE, Walder D, Trottman H, Daley M, et al. (2010): Markers of basal ganglia dysfunction and conversion to psychosis: Neurocognitive deficits and dyskinésias in the prodromal period. *Biol Psychiatry* 68:93–99.
78. Mittal VA, Neumann C, Saczawa M, Walker EF (2008): Longitudinal progression of movement abnormalities in relation to psychotic symptoms in adolescents at high risk of schizophrenia. *Arch Gen Psychiatry* 65:165–171.
79. Bora E (2016): Differences in cognitive impairment between schizophrenia and bipolar disorder: Considering the role of heterogeneity. *Psychiatry Clin Neurosci* 70:424–433.
80. Bortolato B, Miskowiak KW, Köhler CA, Vieta E, Carvalho AF (2015): Cognitive dysfunction in bipolar disorder and schizophrenia: A systematic review of meta-analyses. *Neuropsychiatr Dis Treat* 11:3111–3125.
81. Lynham AJ, Hubbard L, Tansey KE, Hamshere ML, Legge SE, Owen MJ, et al. (2018): Examining cognition across the bipolar/schizophrenia diagnostic spectrum. *J Psychiatry Neurosci* 43:245–253.
82. Jabben N, Arts B, van Os J, Krabbendam L (2010): Neurocognitive functioning as intermediary phenotype and predictor of psychosocial functioning across the psychosis continuum: Studies in schizophrenia and bipolar disorder. *J Clin Psychiatry* 71:764–774.
83. Dalley JW, Robbins TW (2017): Fractionating impulsivity: Neuropsychiatric implications. *Nat Rev Neurosci* 18:158–171.
84. Alexander LM, Escalera J, Ai L, Andreotti C, Febre K, Mangone A, et al. (2017): An open resource for transdiagnostic research in pediatric mental health and learning disorders. *Sci Data* 4:170181.
85. Volkow ND, Koob GF, Croyle RT, Bianchi DW, Gordon JA, Koroshetz WJ, et al. (2018): The conception of the ABCD study: From substance use to a broad NIH collaboration. *Dev Cogn Neurosci* 32:4–7.
86. Zohar J, Nutt DJ, Kupfer DJ, Moller H-J, Yamawaki S, Spedding M, et al. (2014): A proposal for an updated neuropsychopharmacological nomenclature. *Eur Neuropsychopharmacol* 24:1005–1014.
87. Zohar J, Stahl S, Moller H-J, Blier P, Kupfer D, Yamawaki S, et al. (2015): A review of the current nomenclature for psychotropic agents and an introduction to the neuroscience-based nomenclature. *Eur Neuropsychopharmacol* 25:2318–2325.